An hierarchical view on modelling the reliability of a DSRC-link for ETC applications

A. Visser, H.H. Yakali, A.J. van der Wees, M. Oud, G.A. van der Spek, L.O. Hertzberger

Abstract— **For electronic payments, the communication link has to be reliable. Dedicated short range communication is a proposed solution for the automatic debiting of vehicles without disturbing the traffic flow. The requirements on the reliability of such a system are high, which implies that only large scale simulations with a lot of detail are effective to analyse an occasional error. In this article, an hierarchical approach is worked out that allows such simulations of the communication link with a 80% reduction of the computational effort compared to simulation with full detail.**

Keywords— **simulation, modelling, communication, electronic fee collection**

I. Introduction

In the Netherlands Automatic Debiting Systems for traffic will be introduced in the near future. To analyse the reliability of such systems a project is initiated by the Dutch government. The goal of the project is to evaluate the technical feasibility of Automatic Debiting Systems (ADS) for Electronic Toll Collection (ETC) on the Dutch road network. We have designed a modelling and simulation approach for this evaluation project, and developed a software environment to perform these simulations. The environment, called ADSSIM [1], is used by both Ministry government and industry.

In an automatic debiting system on the road network, it is essential that the exchange of information between roadside system (RSS) and the on-board unit (OBU) in a moving vehicle is reliable and fast. This is the task of the dedicated short-range communication system (DSRC), one of the subsystems of the ADS. Other subsystems are used for vehicle detection, co-ordination and license plate registration.

In this paper, a hierarchical approach is introduced to model the reliability of the communication subsystem. At the lower levels, more detail is added to the communication model. We will show the trade-off between reliability of the results and computational effort. As a result of this analysis, insight is gained into the parts of the communication model that are critical for defining the reliability of the system.

Drs. A. Visser, Dr. H.H. Yakali, Dr. M. Oud and Prof. Dr. L.O. Hertzberger are with the University of Amsterdam, department of Computer Science, NL.

Dr. Ir. A.J. van der Wees is with the CMG Den Haag B.V, division Advanced Technology, NL.

Ir. G.A. van der Spek is with the TNO Physics and Electronics Laboratory, NL.

II. Modeling

In order to simulate a complete ADS [2], we have to model the different subsystems [3]. In this article we are only interested in the communication subsystem: the link between the microwave antennas at a gantry above the road (the roadside system) and the small patch antenna (on-board unit) in moving vehicles. Via this link a certain fee that has to be paid for the passage is collected. When the vehicles are not equipped with an OBU, their license plate will be registered, which is a task of the other subsystems of the ADS (detection & registration). The other subsystems are out of the scope of this article.

A communication link for electronic payments has to be reliable. To proof the reliability of such a system, a detailed analysis of the occasional errors is needed. Large scale simulations are well suited for this job. The aim of this article is to find the right level of detail needed for such an analysis.

Therefore, a hierarchical approach is used for modelling the communication. In this article, five communication models will be described with their implementation. Each lower level model contains more details, but is computational more expensive.

The following five communication models are distinguished:

- *Transmitter Geometry Model* is the highest model with the least detail. It provides the spatial distribution of the three volumes in the ADS configuration where communication is possible, not possible or perhaps possible.
- *Transmitter Field Model* provides the spatial distribution of the strength of the electromagnetic (EM) field of the transmitting antennas.
- *Single-Receiver Model* provides the EM vector-field (including amplitude, phase and polarisation) at the receiver of an OBU, which could be direction, phase and polarisation dependent.
- *Single-Vehicle Model* is an extension of the Single-Receiver Model with bonnet reflections and windscreen influences.
- *Multiple-Vehicle Model* is an extension of the Single-Vehicle Model with reflections and disturbances from other vehicles.

In the following section, the different implementations of the five models will be discussed.

The communication system modelled as case-study, is the Philips/Kista system designed in 1990. From this system a large set of measurements is available [4]. Although the system is not completely comparable with the commercial systems currently available, the results of this study are general applicable.

Especially for this article the parameters of the Philips/Kista are tuned in such a way that the communication performance is just enough too exchange the information for the electronic payment. In this way the effect of the different hierarchical models can be seen in a difference of the number of not successful transactions.

III. Implementation

A. Transmitter Geometry model

The 'communication zone' is the area where the transaction takes place for most of the passages. In this area the signals on both downlink and uplink are off such level that a reliable link is guaranteed. Around this zone is an area where the success of the transaction depends on many parameters.

Based on this, we define 'grey' zones (where a more detailed modelling of the communication is needed) next to 'white' zones (where a high level modelling of communication is sufficient).

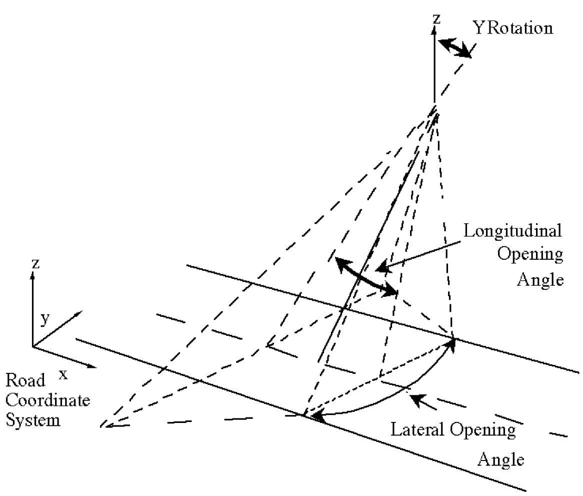

Fig. 1. Definition of a VolumeTriangle

The volumes in the ADS configuration where communication is possible are implemented as so called VolumeTriangles, which include both the white and the grey zones described above. The Philips/Kista system [4] is modelled with the following parameters (Fig. 1):

```
LateralOpeningAngle:         50.0 ; degree
YRotation:                  -69.75; degree
LongitudinalOpeningAngle:  32.25; degree
;TransceiverHeight            5.3 ; meter
```

Fig. 2 gives two cross-sections of this volume: a side view and a top-view. The thick bars in the figure are the measurements performed on the Philips/Kista system in 1990. A thick bar indicate the largest uninterrupted interval where the signal level exceeds a threshold, so that reliable communication is warranted.

a) 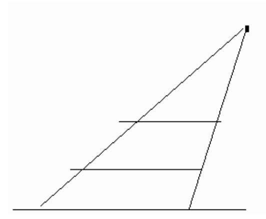	b) 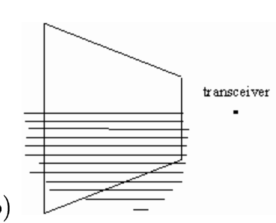
Side view of cross-section VolumeTriangle at the centre ($Y = 0m$) of the footprint (measurements at 1.25 m and 2.65m height)	Top view of cross-section VolumeTriangle at 1.25 meter height (measurements only for $Y \leq 0m$)

Fig. 2. Footprints of the VolumeTriangle and measured uninterrupted interval of signal levels above a certain threshold. The projection of the position of the transceiver is indicated.

The topology of the VolumeTriangle is chosen in such way that uninterrupted signal levels inside the volume can be guaranteed. The only exception is that at the far edges at low height, the location of the communication zone is not correct, although the length of the communication zone is not overestimated.

B. Transmitter Field model

Around the 'white' zone of the Transmitter Geometry Model, there is an area where microwave signals are received, but a successful transaction cannot be guaranteed. The quality of the signal in this 'grey' area depends on many parameters, which can attenuate or amplify the signal. In the Transmitter Field Model, a rough estimation of the microwave signal based on standard mathematical models for the main lobes of the antenna field pattern [5] is made.

In the Transmitter Field Model, it is assumed that the actual power received at a certain location is independent of the orientation of the OBU, and the shape of the vehicle carrying it. These assumptions are quite reasonable. For instance, the difference in signal level between this model and the lower Single Receiver Model, which takes the orientation into account, is in the area directly under the gantry ($X > -5m$), and at the far edges of the communication zone ($|Y| > 3.5m$).

In the Transmitter Field model, we will use the following simple formula to calculate direct path loss that takes into account losses due to distance, azimuth angle and elevation angle:

$$loss(r, \phi, \theta) = loss(r) + loss(\phi) + loss(\theta)$$

where

$$loss(r) = -20log(r)[dB]$$

$$loss(\phi) = \frac{-6}{log(cos(22.5^o))} log(cos(\phi))[dB]$$

$$loss(\theta) = 20log(\frac{sin(K_s sin(\theta - \theta_0)(1 + cos(\theta - \theta_0))}{2K_s sin(\theta - \theta_0)})[dB]$$

and $\theta_0 = 35^o$ and $K_s = 8.87$.

The formulas used for calculating the azimuth and elevation losses are standard mathematical models [5, page 180-185] for the main lobe of moderate and narrow antenna patterns, respectively. The parameters in the azimuth and elevation loss equations are chosen in accordance with the specification of the Philips/Kista system [4, page 13].

In Figure 3 the field obtained from this model (a,b) and the actual measurements (c,d) for different values of the lateral position Y are shown and they match quite well. Since this is a crude model, there are some differences between model and measurements. Notice for instance that there are no sidelobes. The measurements are taken from [4], for an OBU with a 'standard' orientation (elevation angle $\theta_{OBU} = 45^o$, azimuth angle $\phi_{OBU} = 0^o$). For the calculations no OBU orientation is taken into account.

In the images at the top, two curves can be found. Only the upper curves should be compared with the measurements. Validation issues will be discussed more thorough in section IV. Here both calculations and measurements are used to illustrate the impact of the modelled effects. The lower curves represent a pessimistic scenario used to generate the results for section V.

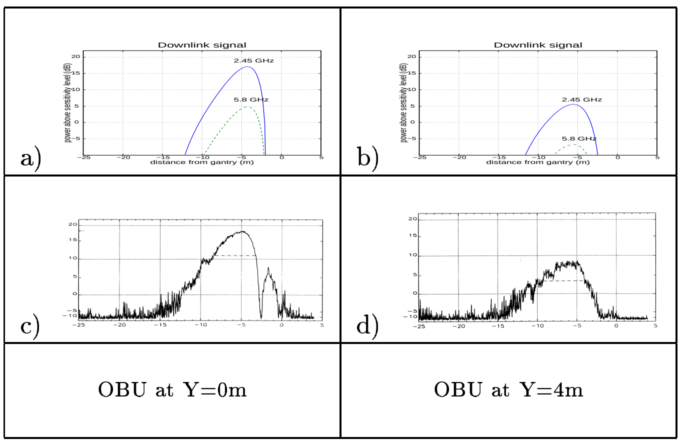

Fig. 3. Calculations and measurements of the received power for two values of Y. The measurements are taken from [4, page A.1 & A.9].

C. Single-Receiver model

On this level, both the transmitter and the receiver antennas are modelled. The antennas are modelled as arrays of patch elements. Although each patch antenna element that emits (or receives) signals has a wide field pattern, by combining the fields of all patches that make up an antenna, narrow antenna patterns can be obtained.

The antennas at the gantry (the so called Road Side Equipment) of the Philips/Kista system contain eight patch elements (array of 4x2). The antenna in the vehicles (on the On Board Unit) contains a single or a double-patch. The next figure shows the side view of both antenna positions with their schematic directional patterns.

The far field model (Carver and Mink [6]) of a linearly polarised rectangular microstrip patch antenna operating

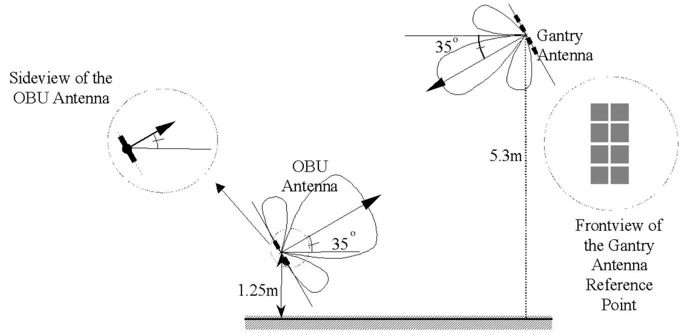

Fig. 4. The single-receiver model for the single patch version of the Philips/Kista system.

in the TM_{10} mode at location P(R,θ,ϕ) is given by the following expressions:

$$E_{\theta,patch}(R,\theta,\phi) = E_{main}(R,\theta,\phi)cos\phi$$

$$E_{\phi,patch}(R,\theta,\phi) = E_{main}(R,\theta,\phi)cos\theta sin\phi$$

$$\begin{aligned} E_{main}(R,\theta,\phi) \quad &= \quad e^{-j(k_0R-\frac{\pi}{2})}\frac{V_0k_0a}{\pi R}cos((ktcos\theta) \\ &sinc(k_0\frac{a}{2}sin\theta sin\phi)cos(k_0\frac{b}{2}sin\theta cos\phi) \end{aligned}$$

where $k = k_0\sqrt{\epsilon_r}$, $k_0 = 2\pi/\lambda_0$, ϵ_r is the dielectric constant and V_0 the voltage applied to the patch. The expressions are formulated in the local spherical coordinate system illustrated in Figure 5. E_θ and E_ϕ denote the field components along the vectors $\hat{u}_\theta$ and $\hat{u}_\phi$ at point P. The field component in the radial direction E_R is zero (in the far field).

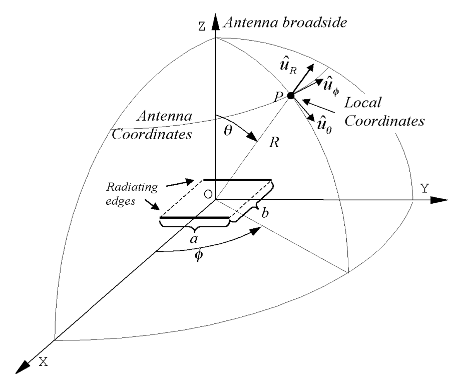

Fig. 5. Geometry for far-field pattern of rectangular microstrip patch.) Philips/Kista system.

In order to generate elliptically polarised waves, we assume that there exists an equivalent second antenna emitting with a 90^o phase difference at the same location, and with its coordinate system rotated 90^o about the z-axis. At broadside the polarisation will be circular, the ellipticity ratio will gradually deviate from one when moving away from broadside ($\theta = 0^o$).

The contribution of all the (eight) patches in the gantry antenna are summed to compute its field pattern at a certain point:

$$E_\theta(R,\theta,\phi) = \sum_{n=1}^{N} \sqrt{P_n} E_{\theta,n}(R,\theta,\phi) e^{i\alpha_{\theta,n}}$$

$$E_\phi(R,\theta,\phi) = \sum_{n=1}^{N} \sqrt{P_n} E_{\phi,n}(R,\theta,\phi) e^{i\alpha_{\phi,n}}$$

where P_n denotes the power level and (α_n the relative phase of the n^{th} patch element. The field components of the gantry array antenna are scaled by the directional sensitivity of the OBU antenna and projected onto the Z=0 (patch) plane of the OBU coordinate system. The OBU of the Philips/Kista system is only responsive to the left-hand circular polarised component in that plane.

With the aid of this detailed and computationally intensive model of the transmitting and the receiving antennas, the amplitude and the phase of the received field can be accurately computed.

Fig. 6 shows the calculated and the measured received power for different angles of the OBU with a single patch antenna. When these plots are compared using the locations of the maxima and minima, it can be seen that they are quite similar.

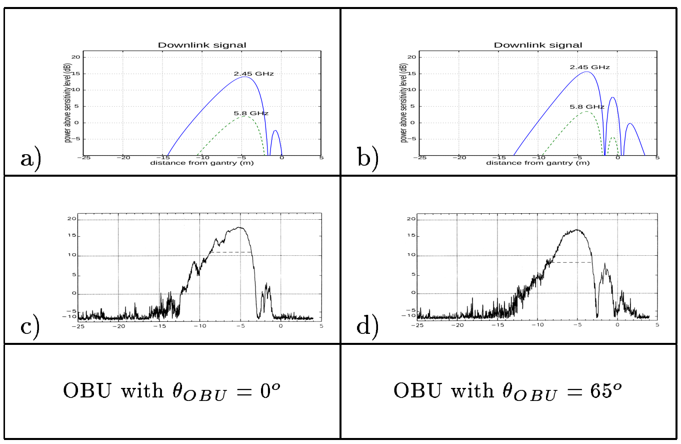

Fig. 6. Calculations and measurements of the received power for two values of OBU orientation θ_{OBU}. The measurements are taken from [4, page A.13 & A.14].

D. Single Vehicle model

In the previous model, the vehicle that carries the OBU antenna is not taken into account. The windscreen and the bonnet are the two parts of the vehicle, which have the strongest influence on the communication link. The windscreen influence is currently modelled as a constant attenuation. From the bonnet, reflections can be expected. Circular polarised fields change the sign (and ellipticity ratio) of their polarisation when they reflect off a metallic surface. Since the receiver antennas are sensitive to only one type of polarisation, the interfering effect of reflections from the bonnet is limited. However, the effect is not completely absent due to two reasons: the field is not perfectly circularly polarised in all directions and each reflection path and the direct path have a different length and loss. In the Single-Vehicle model, only the bonnet reflection is taken into account. A simple form of ray tracing is performed, based on specular reflections only (see Figure 7).

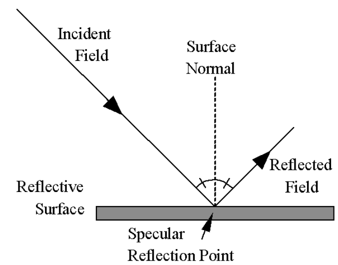

Fig. 7. Specular reflection is used in ray tracing

In the right hand side of figure 8, the effect of reflection can be seen.

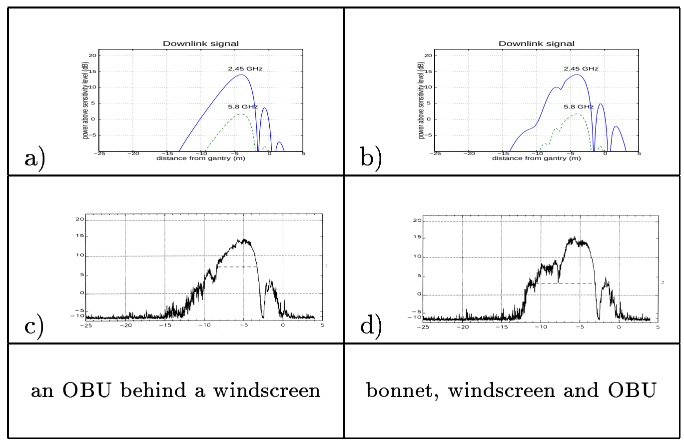

Fig. 8. Calculations and measurements of the received power at Y=0 and $\theta_{OBU} = 45^o$ for an vehicle with and without a bonnet. The measurements are taken from [4,page A.16 & A.17].

E. Multiple Vehicle model

In the multiple vehicle model the vehicles that surround the communicating vehicle are also taken into account. The surrounding vehicles can have three effects:

- The communication-link can be blocked.
- The communication-link can be disturbed by (multiple) reflections.
- The communication-link can be disturbed by diffraction (edge effect).

In ADSSIM, only the first two effects are modelled, since the last one can be handled by simply checking the level of occlusion. A double-reflection can have a strong impact on the received signal. A circularly polarised field that is reflected twice on a metal surface has a strong co-polar component, which will interfere with the field received via the direct path. A realistic scenario for a double reflection is a beam that is first reflected by the sideplane of a truck driving next to a passenger car, and then, bounces via the bonnet of the passenger car to the OBU. With the same ray tracing technique the reflection via a sideplane and a bonnet is studied. This yielded the following field patterns:

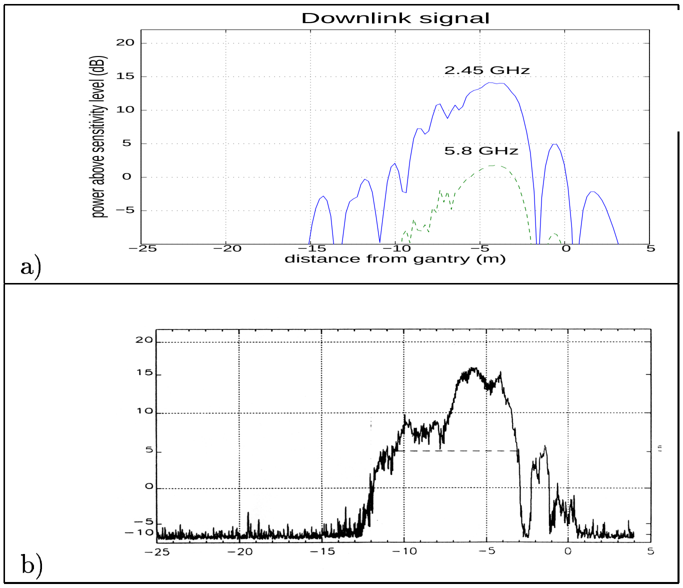

Fig. 9. Calculation and measurement of the received power at Y=0 and $\theta_{OBU} = 45^o$ for a vehicle with a bonnet driving next to a large truck. The measurement is taken from [4, page A.25].

Figure 9.b is not significantly different from figure 8.d, which means that the presence of a large truck doesn't influence the measured signal quality. Note that, the measurements were performed at a frequency of 2.45 GHz, so that the reflecting surfaces were rather small in terms of wavelength and only little interference may result. More results will be presented in the next section for the wavelength of 5.8 GHz, in which case the surfaces are relatively larger and the effect of double reflections is more visible.

IV. Validation

In the previous section calculations based on five models are compared with the detailed measurements performed on the Philips/Kista system in 1990. The comparison is presented in Figure 3, 6, 8 and 9.

Furthermore, our results are also checked by comparison with other simulation tools. The field pattern of a linearly polarised patch element described in the single-receiver model is compared with field pattern of a patch element defined in Personal Computer Aided Antenna Design program (PcAAD version 2.1. [7]). Fig. 10 shows the plots generated for both programs, the field patterns fit exactly.

Further comparisons have been made using the antenna analysis program Ensemble [8], which is capable of analysing the effect of patch antenna feeding. For this comparison, a 4 (rows) by 2 (columns) array antenna with circularly polarised square patch elements is used. A comparison of the results of the Transmitter Field Single Receiver Model with those of Ensemble yielded the conclusion that our model can calculate correctly the amplitude of the field. However, Ensemble produced a different phase pattern, due to the delays in the feeding lines to the different patches.

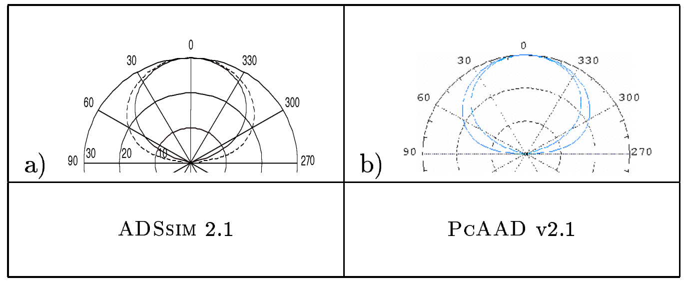

Fig. 10. Field patterns of linearly polarised square patch antenna obtained with both PcAAD v2.1 and our algorithm. In both cases, the single square patch had a length of 2.65cm, substrate thickness of 0.265cm, operating frequency of 5.8GHz and dielectric constant of 1.

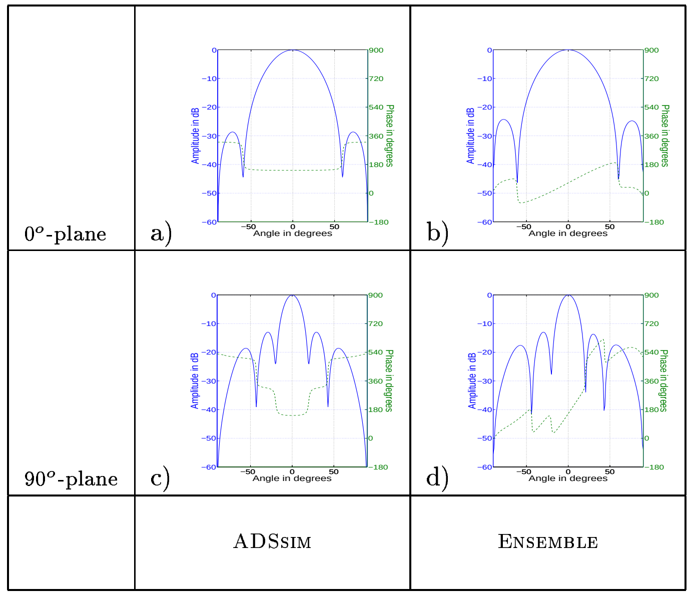

Fig. 11. Array antennas field patterns obtained with our Transmitter Field Single Receiver Model (a,c) and Ensemble (b,d) for two planes through the z-axis. Both programs used a 4 by 2 array antenna with circularly polarised square patches with length of 2.65cm, substrate thickness of 0.265cm, operating frequency of 5.8GHz and dielectric constant of 1. (Solid line: amplitude, dashed line: phase.)

The ray-tracing algorithm used in the single- and multiple-vehicle models was validated with another the simulation program called Rapport (Radar signature Analysis and Prediction by Physical Optics and Ray Tracing) [9]. This program combines ray tracing with Physical Optics. In the Physical Optics approach, a ray is not reflected in a single direction, but has a directivity pattern due to scattering. In order to increase the influence of reflections, an OBU patch antenna with directional sensitivity in front of the patch surface is used. The results obtained by both models are shown in Figure 12.

As can be seen from the figure they compare quite nicely. The main difference can be seen around X=-5m. Our model shows a sharp change in the interference pattern, because the specular reflection point falls of the bonnet. In contrast, the change in the interference pattern in Rap-

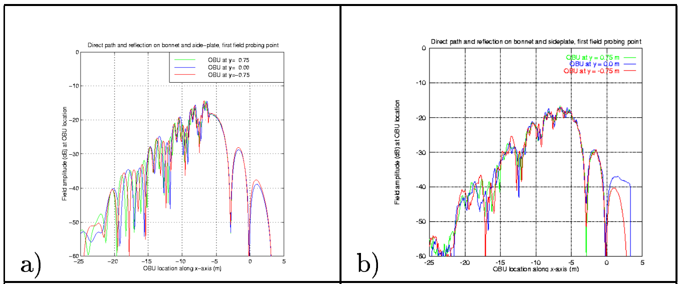

a sideplane, bonnet and OBU in ADSSIM	a sideplane, bonnet and OBU in RAPPORT

Fig. 12. The received power at Y=0, Plots show the combined effect of the direct path, the path reflected at both the sideplane of the truck and the bonnet, and the path with a single reflection at the bonnet.

PORT is smooth, due to the diffused reflection. This difference becomes more pronounced for smaller bonnets.

V. RESULTS

In this section, we will distinguish three different outcomes of the transaction: no transaction, an incomplete transaction and a complete transaction. For each hierarchical model, we will predict the number of cases and record the computational price paid for the increasing level of detail.

In the table II one can see that the detailed Multiple Vehicle Model needs more than 100 times the running time of the Transmitter Geometry Model. All calculations where performed on Sparc Ultra 10 workstations with a 300 MHz processor. The simulation results are based on 10.000 passages of vehicles, all equipped with an OBU.

The Single Receiver Model has better results compared to both Transmitter models for two reasons. The first reason is related the RSS antenna pattern under the gantry. The Transmitter Field model contains only the main lobe. Yet, for many transactions, a message has to be exchanged when the OBU is between the main lobe and the first sidelobe. For the Single Receiver model, the message is exchanged in the sidelobe, after a number of retries. In the Transmitter Field model there is no sidelobe, so the transaction is not completed. Detailed analysis showed that the side lobe is involved in 13% of the transactions. The second reason is that the Transmitter model rejects all communication when the Bit Error Rate is worse than 10^{-6}. In practice, messages can still be exchanged for rates $> 10^{-6}$, although retries become likely. This effect contributes to successful transactions for 36% of the passages.

The percentage of completed transactions predicted by both Vehicle Models is lower than that of the Single Receiver Model. In this model, the receiver is a free-floating device in the air, windscreen and reflections are not taken into account. The influence of the reflections on the received signal can be both positive and negative. For instance, the variations in the signal level obtained using the Single Vehicle Model are between -3.3 and +12.8 dB, and between -41.4 and +35.8 dB for the Multiple Vehicle Model, compared to the Single Receiver Model. On the average, the reflection increased the power level in the receiver.

The fact that the Transmitter Field model Model is more stringent makes it possible to use this model as a filter for a more detailed model. When the Transmitter model Field Model predicts a successful transaction, there is no need to perform any detailed processing. Only the rejected cases ($\tilde{3}5\%$) require further detailed analysis. With this filtering, not more than 20% of the running time is needed, without a significant loss of accuracy (Table III).

Although the hierarchical approach, proposed in this article, requires more effort for the modeller, the advantage is that simulations are performed in less time. Furthermore, insight is gained into which assumptions have the greatest influence on the performance of the communication link.

VI. CONCLUSIONS

In this paper, a hierarchical approach to model the reliability of the communication link is introduced and worked out. We have shown that the communication link can be modelled in five hierarchical levels. At each level, more detail is added to the communication model. More detail means more computational effort, and more effort to find (and calibrate) the required parameters. Yet, these details can have major impact on the performance of the communication link. In order to bring out the effect of our hierarchical model clearly, a system with a weak communication link was chosen.

Our study has shown that, although there are five logical hierarchical communication reliability models, there is no need to use all of them sequentially. We have shown that only two of them are sufficient to obtain a detailed analysis:
1. the Transmitter Field Model (the spatial distribution of the strength of the electromagnetic field of the transmitting antennas) serves to decide whether more detail is necessary, and
2. the Multiple Vehicle Model (the reflected and disturbed electromagnetic vector-field as received by the OBU) to perform this detailed analysis.

This reduced the computation time to 20% without a significant loss of accuracy.

This approach makes it possible to simulate the performance of the short-range communication link for millions of vehicle passages, in a comparatively short time. This is needed, to demonstrate that short-range communication is a reliable way of data exchange. In large-scale Intelligent Transportation projects, as the Rekeningrijden project in the Netherlands [10], the number of passages is so large and the requirements so high, that failure events with a low probability must be accurately estimated. Simulation can give such an estimate, based on models validated on small-scale experiments.

ACKNOWLEDGMENTS

This research was performed with the financial backing of the Dutch Ministry of Transport, Public Works & Wa-

TABLE I

Communication results for the different hierarchical levels, without contribution of any other level.

	No transaction	Incomplete transaction	Complete transaction	Running time
Transmitter Geometry model	41.68%	0.00%	58.32%	0h03
Transmitter Field model	34.53%	0.01%	65.46%	0h08
Single-Receiver model	0.00%	2.46%	97.54%	3h21
Single Vehicle model	0.03%	8.73%	91.24%	4h45
Multiple Vehicle model	0.16%	9.71%	90.13%	5h33

TABLE II

Communication results for the different hierarchical levels, with filtering by the Transmitter Field Model.

	No transaction	Incomplete transaction	Complete transaction	Running time
Single-Receiver model	0.01%	1.98%	98.01%	0h33
Single Vehicle model	0.01%	8.27%	91.72%	0h45
Multiple Vehicle model	0.01%	8.77%	91.22%	1h04

ter Management, for the 'Rekeningrijden' project. Special thanks to F.C.A. Groen and M. van den Akker for the careful proof-reading. M. Bergman (University of Amsterdam) and I. van Megen (CMG Den Haag B.V.) were instrumental in their support of the ADSsim environment. L.J. van Ewijk and F.P. van der Wilt (TNO Physics and Electronics Laboratory) helped us by validating our results with the simulation environments available at their site.

References

[1] A.G. Hoekstra, G.R. Meijer, and L.O. Hertzberger, *ADS-SIM: a generic simulation environment to evaluate and design Automatic Debiting Systems*, Proceedings 14th ITS Conference, Berlin 1997.

[2] A.G. Hoekstra, L. Dorst, M. Bergman, J. Lagerberg, A. Visser, H. Yakali, F. Groen and L.O. Hertzberger, *High Performance Discrete Event Simulations to evaluate Complex Industrial Systems. The case of Automatic Debiting System for Electronic Toll Collection on Motor Highways*, High Performance Computing and Networking, Eds. Bob Hertzberger and Peter Sloot, Lecture Notes in Computer Science 1225 (Springer), pp.41-50, 1997.

[3] L. Dorst, A. Hoekstra, J.M. van den Akker, J. Breeman, F.C.A. Groen, J. Lagerberg, A. Visser, H. Yakali, L.O. Hertzberger, *Evaluating Automatic Debiting Systems by modelling and simulation of virtual sensors*, IEEE Instrumentation and Measurement Magazine, June 1998, vol.1, no.2, pp. 18–25.

[4] A.J.A. Bruinsma, J.C. Henkus, F.J. van der Mark, *Experiments with prototype infrared and microwave datatransmission equipment for Rekening Rijden*, TNO report TPD-HAI-RPT-90-31, June 1990.

[5] R.C. Johnson, *Designer Notes for Microwave Antennas*, Artech House, Boston, 1991.

[6] K.R. Carver and J.W. Mink, *Microstrip antenna technology*, IEEE Trans. Antennas Propagat.; vol AP 29, pp. 2-24; Jan. 1981.

[7] D. M. Pozar, PcAAD - *Personal Computer Aided Antenna Design for Windows, version 3.0*, Antenna Design Associates, Inc., 1996.

[8] R.C. Hall and D.I. Wu, *Design, Review & ID Array Synthesis, User's Guide, Volumes 1 and 2*, Boulder, Colorado, Boulder Microwave Technologogies, Inc, March 1997

[9] L.J. van Ewijk and G.A. van der Spek, *Simulation of reflection effects for a dedicated short range microwave communication system*, TNO report FEL-8-C168, July 1998, submitted for publication in IEE Proceedings Communications.

[10] D.P. van Wijk and W.J. Jägers, *Evaluating the performance of EFC systems*, Proceedings Int. Conf. On Transportation in the Next Millennium, Singapore, 9-11 September 1998.

Arnoud Visser studied physics at the Univeristy of Leiden, The Netherlands, where he performed investigations in the field of nonlinear optics. At the University of Amsterdam since 1991, he participated in several international projects (ESPRIT, ESTEC) for the Computer Science Department.

Hüseyin Hakan Yakalı has M.Sc.(1989) and Ph.D.(1994) degree(s) from the Department of Electrical Engineering at Florida Atlantic University in Boca Raton, Florida. His Ph.D. thesis was on extraction of 2-D visual cues for autonomous vehicle control. In 1994, he has started working as a Post Doctorate at the University of Amsterdam, The Netherlands, where he is working as a researcher since 1996. His areas of interest are in robotics, controls and autonomous systems .

Aad-Jan van der Wees received his master's degree in applied mathematics in 1980 and his doctor's degree in technical sciences in 1988. Since 1986 he works for CMG Advanced Technology. At present he is a senior consultant at the Netherlands Ministry of Transport. His work focuses on digital simulation methods for the evaluation of Automatic Debiting Systems.

Mireille Oud received her Master's degree in Applied Physics in 1989 and her PhD in 1993. Her PhD thesis was on Ion-atom collisions. Currently she is working as Post Doctorate at the University of Amsterdam, e.g., the signal processing of asthmatic respiration sounds.

Gerard A. van der Spek (M'68) received the M Sc degree in electrical engineering from Delft University of Technology, the Netherlands, in 1961. Since 1960 he has worked for TNO Physics and Electronics Laboratory (TNO-FEL), The Hague, on digital datatransmission, signal processing, sonar and radar. Presently he is a senior advisor.

Louis O. Hertzberger received his Master's degree in experimental physics in 1969 and his PhD in 1975, both from the University of Amsterdam. From 1969 till 1983 he was a staff member in the High Energy Physics group, later the NIKHEF-H (Dutch Institute for Nuclear and High Energy Physics). As an instrumental physicist he was involved in a number of experiments mostly at CERN, Geneva. In 1983 he became a full professor in computer science at the University of Amsterdam. His current research is in the field of High Performance Computer Systems as well as complex- and autonomous systems research. He participated, among others, in a large number of parallel computer projects with industries such as Philips etc.